Morphometry of the ciliary body and systemic inflammation in neovascular glaucoma secondary to diabetic retinopathy and/or retinal vein occlusion

Guzun O.V., Zadorozhnyy O.S., Sytnikova V.O., Konovalova N.V., Kovalchouk A.G.

[1] SI «The Filatov Institute of Eye Diseases and Tissue Therapy of the National Academy of Medical Sciences of Ukraine» Odesa (Ukraine)

[2] Odesa National Medical University, Odesa (Ukraine)

Морфометрія циліарного тіла та системне запалення при вторинній неоваскулярній глаукомі внаслідок діабетичної ретинопатії та оклюзії вен сітківки

Гузун О. В. [1], канд. мед. наук; **Задорожний О. С.** [1], д-р мед. наук; **Ситнікова В. О.** [2], д-р мед. наук, професор; **Коновалова Н. В.** [2], д-р мед. наук; **Ковальчук О. Г. 1,** канд. мед. наук

[1] ДУ «Інститут очних хвороб та тканинної терапії ім. В.П.Філатова НАМН України», Одеса (Україна)

[2] Одеський національний медичний університет, Одеса (Україна)

Abstract

Purpose: *To assess ultrasound biomicroscopy (UBM)-based morphometric features of the ciliary body (CB) in patients with neovascular glaucoma (NG) secondary to diabetic retinopathy (DR) anf/or retinal vein occlusion (RVO), and determine their relationships with the stage of rubeosis (according to the Weiss grading system) and systemic inflammation indices (Systemic Immune-Inflammation Index [SII], Systemic Inflammation Response Index [SIRI], and Aggregate Index of Systemic Inflammation [AISI]).*

Material and Methods: *Totally, 160 eyes were included in the study. Of these, 126 had NVG (65 eyes with NVG secondary to DR and 61 eyes with NVG secondary to RVO), and 34 eyes were used as controls. UBM was used to determine CB thickness at a point 1-mm posterior to the sclera spur (CBT1) and maximum CB thickness (CBTmax). The stage of rubeosis was determined according to the Weiss grading system. Spearman rank correlation was used for associations. Multivariate regression analysis with CBTmax as a dependent variable was performed to determine independent predictors of CB thickening.*

Results: *CB thickness was significantly greater in eyes with NVG (1.17–1.50 mm; CBTmax as much as 1.64–1.66 mm) than in controls (CBT1 = 0.82 mm). The greatest values were seen in NVG secondary to RVO (CBT1 = 1.39 mm; CBTmax = 1.66 mm) and NVG secondary to DR with a duration ≤ 5 years (CBT1 = 1.25 mm; CBTmax = 1.63 mm). These values were actually twice as high as normal values, supposing the formation of a hypervoluminous phenotype. Thinning of the CB (CBT1 = 0.57–0.64 mm; CBTmax = 0.74–1.00 mm) was observed in NVG secondary to DR with a duration > 5 years. Systemic indices increased with the stage of rubeosis: SII was increased more than twofold, AISI was increased 2.5–3-fold, and SIRI was increased 1.3–2-fold compared with controls.*

Conclusion: *NVG is accompanied by stage-dependent morphometric changes in the CB, which is manifested by the formation of a hypervoluminous or atrophic phenotype depending on disease etiology and duration. CB thickness demonstrates a close relationship with systemic immune inflammation and rubeosis activity, which highlights its clinical and potential prognostic value.*

Keywords: *neovascular glaucoma, diabetes mellitus, ultrasound biomicroscopy, ciliary body thickness, systemic inflammation, rubeosis, iris, glaucoma, ciliary body*

DOI: https://doi.org/10.31288/Ukr.j.ophthalmol.202614654

UDC: 617.7

Corresponding Author: Olga V. Guzun, SI «The Filatov Institute of Eye Diseases and Tissue Therapy of the National Academy of Medical Sciences of Ukraine», 49/51 Frantsuzkyi Bulvar, Odessa 65015, Ukraine. Email: olgaguzun24@gmail.com

Received 2026-02-02

Accepted 2026-02-13

Cite this article as: Guzun O.V., Zadorozhnyy O.S., Sytnikova V.O., Konovalova N.V., Kovalchouk A.G.Morphometry of the ciliary body and systemic inflammation in neovascular glaucoma secondary to diabetic retinopathy and/or retinal vein occlusion. Ukrainian Journal of Ophthalmology . 2026;1:46-54.

Резюме

Мета. *Оцінити морфометричні особливості циліарного тіла (ЦТ) за даними ультразвукової біомікроскопії (УЗБ) у пацієнтів з неоваскулярною глаукомою (НВГ), асоційованою з діабетичною ретинопатією (ДР) або оклюзіями вен сітківки (ОВС), та визначити їхній зв'язок зі стадією рубеозу за Weiss і системними імунозапальними індексами крові (SII, SIRI, AISI).*

Матеріал і методи. *У дослідження включено 160 очей: 126 очей з НВГ (65 – на тлі ДР, 61 – після ОВС) та 34 ока контрольної групи. За допомогою УЗБ визначали товщину ЦТ на рівні 1 мм позаду склерального шпора (CBT1) і максимальну товщину ЦТ (CBTmax). Стадію рубеозу оцінювали за класифікацією Weiss. Кореляційний аналіз виконували з використанням Spearman's rank. Для визначення незалежних предикторів потовщення ЦТ застосовано багатофакторний лінійний регресійний аналіз із CBTmax як залежною змінною.*

Результати. *У пацієнтів з НВГ товщина ЦТ достовірно перевищувала показники контролю (CBT1 = 0,82 мм) і досягала 1,17–1,50 мм, а CBTmax – до 1,64–1,66 мм. Найвищі значення зафіксовано при постоклюзійній НВГ (CBT1 = 1,39 мм; CBTmax = 1,66 мм) та при НВГ на тлі ДР тривалістю ≤5 років (CBT1 = 1,25 мм; CBTmax = 1,63 мм), що фактично відповідає подвоєнню фізіологічних показників і дозволяє припустити формування гіпероб'ємного фенотипу. При ДР понад 5 років спостерігалося витончення ЦТ (CBT1 = 0,57–0,64 мм; CBTmax = 0,74–1,00 мм). Системні індекси зростали зі стадією рубеозу: SII – більш ніж у 2 рази, AISI – у 2,5–3 рази, SIRI – у 1,3–2 рази порівняно з контролем.*

Висновки. *НВГ супроводжується стадійно залежними морфометричними змінами циліарного тіла, що проявляється формуванням гіпероб'ємного або атрофічного фенотипу залежно від етіології та тривалості захворювання. Товщина ЦТ демонструє тісний зв'язок із системним імунозапальнням і активністю рубеозу, що підкреслює її клінічну та потенційну прогностичну цінність.*

Ключові слова: *неоваскулярна глаукома; цукровий діабет; ультразвукова біомікроскопія; товщина циліарного тіла; системне запалення; рубеоз, райдужка, глаукома, циліарне тіло.*

Introduction

Neovascular glaucoma (NVG) represents one of the most severe forms of secondary glaucoma and develops due to severe retinal ischemia with excessive expression of antiangiogenic factors, first of all vascular endothelial growth factor (VEGF) [1]. The most common causes are still proliferative diabetic retinopathy (PDR; 33%) and retinal vein occlusion (RVO; 33%). The etiology-based distribution described in 1971 is still relevant, despite a substantial improvement in insights into the pathogenetic mechanisms of NVG [2, 3].

The techniques for anterior segment imaging differ in their capabilities. Optical coherence tomography (OCT) enables an objective precision assessment of the status of the retina, cornea and anterior chamber angle. Along with fluorescein angiography, optical coherence tomography anhiography enables identifying and quantitatively assessing neovascularization of the iris and of the iridocorneal angle, and tracking the regression of rubeosis after anti-VEGF therapy [4]. Infrared transillumination of the eye facilitates determining the width of the shadow of ciliary body (CB) structures on the sclera [5]. These techniques, however, do not enable comprehensively assessing the structure and dimensions of the CB, the location of ciliary processes and the anatomy of the angle. Doppler ultrasound is used for the analysis of blood flow in ocular arteries. The potential for impedance oculopneumoplethysmography in diagnosing microvascular ciliary body ischemia has been substantiated [6], but these works do not provide morphometric data on the CB.

Ultrasound biomicroscopy (UBM), however, enables high-resolution imaging of the deep structures of the anterior segment (e.g., the CB and the iridocorneal angle), irrespective of the transparency of the cornea and the presence of hyphema, which makes it an essential imaging technique in the assessment of severe ischemic and neovascular conditions [7]. It provides a detailed assessment of the configuration and morphometrics of the CB, location of the iris root, status of the anterior chamber angle, and extension of the peripheral anterior synechiae [8, 9].

The morphological changes in the anterior segment in NVG principally differ from those in primary angle-closure glaucoma (PACG) [10]. The mechanisms of pupillary block, iris plateau and lens swelling are typical for PACG [11, 12], whereas ischemic atrophy of the iris stroma, active neovascularization, tractional deformations of the iridocorneal angle and formation of massive peripheral anterior synechiae are typical for NVG [10]. However, in spite of significant interest in the morphology of the anterior chamber angle and iris in NVG, quantitative morphometric characteristics of the CB are still insufficiently investigated.

Chronic low-grade inflammation plays an important role in the development of microvascular diabetic complications, which causes an increasing interest in studies on immune inflammation indices, particularly Systemic Immune-Inflammation Index (SII), Systemic Inflammation Response Index (SIRI) and Aggregate Index of Systemic Inflammation (AISI). Integral hematological indices (particularly SII, SIRI and AISI) calculated on the basis of peripheral blood formula are increasingly used for assessment of systemic inflammatory response and immune status [13, 14, 15, 16, 17]. These indices reflect the balance between neutrophil and monocyte inflammation and lymphocyte regulation and are considered to be the markers of systemic low-grade inflammation.

Even after the achievement of long-term glycemic compensation, inflammatory lesion in diabetes can be maintained and become chronic and partially irreversible [18]. In this context, AISI (also known as pan-immune inflammation value [PIV]), has been actively investigated in diabetic retinopathy (DR) [13, 14]. Some studies stressed the advisability of determining systemic inflammation biomarkers for the clarification of the role of inflammation in the pathogenesis of DR and the prediction of the risk and severity of DR [13, 15, 19, 20].

Similar relationships have been described in RVO: SII was significantly higher in patients with RVO than controls [21], and young patients with RVO exhibited high SIRI, NLR and SII [22]. This indicates a systemic nature of inflammatory response in ischemic retinal lesions.

Taking into account the key role of ischemia, VEGF-mediated neovascularization and the inflammatory cascade in the pathogenesis of NVG, it is advisable to use a complex approach involving UBM of the ciliary body and assessment of the intraocular pressure (IOP), the grade of rubeosis (according to the Weiss grading system) and systemic immune-inflammation indices (SII, SIRI, and AISI). This approach will enable quantitatively assessing the relationship between systemic inflammation and morphological changes of the CB and clarifying its role in the formation of the morphological phenotype in secondary NVG.

The purpose of this study was to assess ultrasound biomicroscopy (UBM)-based morphometric features of the ciliary body (CB) in patients with neovascular glaucoma (NG) secondary to diabetic retinopathy (DR) anf/or retinal vein occlusion (RVO), and determine their relationships with the grade of rubeosis (according to the Weiss grading system) and systemic immune-inflammation indices (SII, SIRI, and AISI).

Material and Methods

Study Design: This study was designed as a prospective clinical analytical study aimed at determining the structural characteristics of the anterior segment and their relationship with systemic inflammation markers in patients differing in NVG etiology, IOP and the grade of rubeosis according to the Weiss grading system.

Study sample: Subjects were 160 patients (160 eyes). These eyes were divided into three groups: group 1 of 65 eyes with NVG secondary to PDR, group 2 of 61 eyes with NVG secondary to RVO, and group 3 (controls) of 34 eyes without iris rubeosis or secondary glaucoma. Patients were examined and treated at SI "The Filatov Institute of Eye Diseases and Tissue Therapy of the National Academy of Medical Sciences of Ukraine".

Eyes with uveitis, trauma, history of filtration surgery, angle-closure glaucoma, NVG secondary to other etiology, NVG in the presence of a Weiss grade 4, or the presence of epibulbar scars preventing correct imaging with UBM were excluded from the study.

Ultrasound Biomicroscopy: We used the Aviso ultrasound system (Quantel Medical; Cournon d'Auvergne, France) having interchangeable probes with transducer frequencies of 50 MHz to 80 MHz (axial resolution: up to 20-25 μm; lateral resolution: up to 40 μm), and meeting the requirements for precise structural measurements of the anterior chamber angle and CB [23]. Subjects were examined supine. Anesthetic and contact gel was applied topically, and a standard scleral eyecup was inserted under the eyelids according to the technique described by Ren and colleagues [9]. UBM was performed in four quadrants (superior, inferior, nasal, and temporal). For each quadrant, a series of longitudinal and transverse cuts was obtained in the iris root, ciliary processes and pars plana. Image quality was assessed using the following parameters: presence of clear margins of the CB, absence of artifacts, and stable scanner position. CB thickness at a point 1-mm posterior to the sclera spur (CBT1) was measured perpendicularly to the inner sclera contour and the average of three measurements was used for the analysis. Maximum CB thickness (CBTmax) for each quadrant was measured as the largest distance from the posterior contour of ciliary processes to the inner sclera, and the average of measurements in the four quadrants was used for the analysis.

The eyes were all classified as to the grade of neovascularization of the iris according to the system devised by Weiss and Gold: Grade 1: Fine iris new vessels at the pupillary zone or crossing the trabecular meshwork, without synechiae <2 quadrants; Grade 2: Iris new vessels at the pupillary zone or crossing the trabecular meshwork, without synechiae >2 quadrants; Grade 3: Iris new vessels at the pupillary zone and ciliary zone with peripheral anterior synechiae 1-3 quadrants; Grade 4: Apparent new vessels at the ciliary zone with extensive peripheral anterior synechiae >3 quadrants [24].

Goldmann applanation tonometry was used to measure IOP. Iridocorneal angle configuration (open or closed), neovascularization grade, and the presence and extension of anterior synechiae were assessed during gonioscopy.

Systemic inflammation indices: These indices were calculated from complete blood counts.

SII = PLT × NEU / LYM;

SIRI = NEU × MON / LYM;

AISI = NEU × MON × PLT / LYM.

The indices were used as integral markers of systemic pro-inflammatory activity.

Ethical standards: This study was conducted in accordance with ethical principles set out in the Declaration of Helsinki and Good Clinical Practice, and was approved by the Bioethics Committee of SI "The Filatov Institute of Eye Diseases and Tissue Therapy of the National Academy of Medical Sciences of Ukraine" (minutes no. 4/2024). Informed consent was obtained from all subjects. Data were depersonalized for confidentiality reasons. Manipulations were within the scope of routine ophthalmological practice.

Assessment criteria

Primary assessment criteria included UBM-based morphometric parameters of the CB: CB thickness at a point 1-mm posterior to the sclera spur (CBT1) and maxi-

mum CB thickness (CBTmax). Primary assessment criteria were analyzed taking into account NVG etiology (PDR vs RVO), the grade of rubeosis according to the Weiss grading system, and duration and stage of DR.

Secondary assessment criteria included clinical and biological characteristics of neovascularization activity and the systemic component of this process: IOP level, the grade of rubeosis according to the Weiss grading system, duration of major disease (PDR or RVO) and SII, SIRI and AISI. The characteristics above were used to analyze their relationships with morphometric parameters of the CB and assess interactions between the structure and inflammation in NVG.

Statistics: JASP software (JASP Team, Amsterdam, Netherlands; Version 0.19.2) was used for analysis. Nonparametic statistic methods were used because quantitative variables did not follow a normal distribution. Data are presented as median (Me) and interquartile range (IQR). Nonparametric Mann-Whitney U-test or Kruskal-Wallis test with post-hoc analysis as required were used to compare independent groups. Spearman rank correlation coefficient (rs) was used to find the associations between quantitative variables. Correlation strength was interpreted using standard thresholds. The level of significance was set at $p < 0.05$.

Results

UBM measurements indicated that, in eyes with NVG, there were changes in anterior segment morphology associated with the grade of rubeosis and systemic inflammation parameters (Fig. 1).

Ciliary body morphometry in patients with NVG

There was a statistically significant difference in UBM measurements of CB thickness depending on the etiology of NVG, Weiss grade of rubeosis and duration of the pathological process (Table 1).

In all grades of rubeosis, CB thickness was smaller in patients with NVG/PDR (CBT1 = 1.15 (0.62–1.30) mm; CBTmax = 1.50 (0.84–1.63) mm) compared to those with NVG/RVO (CBT1 = 1.39 (1.23–1.49) mm; CBTmax = 1.66 (1.58–1.75) mm; $p < 0.000$), indicating different morphological CB phenotypes in eyes with different NVG etiology.

Rubeosis grade analysis showed that morphometric parameters of the CB are characterized by grade-to-grade differences, with a tendency to increase in CB thickness with the progression of rubeosis (Table 1).

Additionally, there was a clear association of morphometric parameters of the CB with the duration of PDR. CB thickness was markedly increased (CBT1 = 1.25 (1.20–1.40) mm; CBTmax = 1.63 (1.58–1.65) mm) in patients with PDR duration shorter than 5 years (58 (55–60) months), and statistically significantly decreased (CBT1 = 0.61 (0.57–0.64) mm; CBTmax = 0.76 (0.74–0.89) mm; $p < 0.000$) in those with PDR duration longer than 5 years, which reflects structural transformation of the CB depending on the duration of the disease. The relationship between CB thickness, rubeosis grade and PDR duration is shown in Fig. 2.

Therefore, based on the data obtained, it may be supposed that, in eyes with NVG due to PDR, morphometry of the CB has a phase nature: a swelling-hypervoluminous

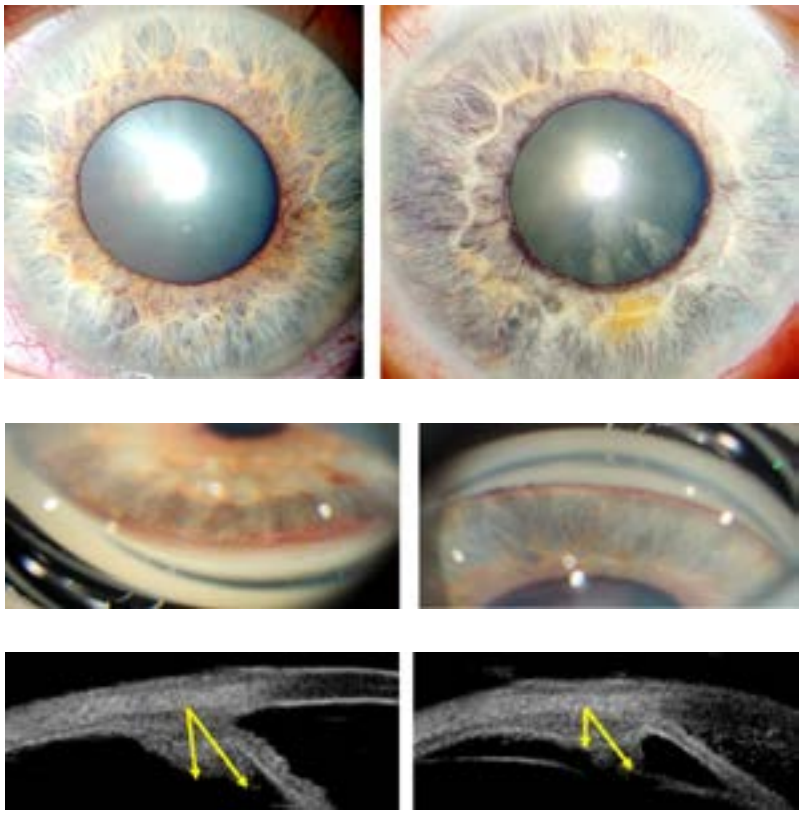

Fig. 1. Photographs of a 58-year-old patient having retinopathy with a type 2 diabetes duration of 5 years; (A, B, C), the right eye; (D, E, F), the left eye. Note neovascularization of the pupillary margin of the iris (A) OD and neovascularization of the iris and complicated cataract (D) OS. Gonioscopy of the anterior chamber angle shows an open iridocorneal angle with visualization of all structures and fine iris new vessels crossing the trabecular meshwork, without synechiae <2 quadrants (grade 1 rubeosis according the Weiss grading scheme) OD (B) and an irregular anterior chamber angle open in two quadrants, iris new vessels at the pupillary zone and ciliary zone with peripheral anterior synechiae 1-3 quadrants (grade 3 rubeosis according the Weiss grading scheme) OS (E). UBM of the ciliary body shows CBT1 of 1.2 mm, CBTmax of 1.6 mm, a massive contour markedly shifted anteriorly, with a dense echogenic structure and an anterior uveal displacement OD (C) and CBT1 of 1.11 mm, CBTmax of 1.3 mm, with a reduced contour and decreased echogenicity at the ciliary processes OS (F). Transscleral cyclophotocoagulation was performed. Note local atrophy of ciliary processes.

Table 1. Structural and systemic inflammation characteristics in neovascular glaucoma (NVG) depending on the etiology and Weiss grade of rubeosis

Characteristic	Controls n=34	Weiss 1		Weiss 2		Weiss 3	
		PDR n=29	RVO n=25	PDR n=25	RVO n=27	PDR n=11	RVO n=9
	Me (IQR);						
CBT_1, mm	0.82 (0.7–0.86)	1.2 (0.62–1.24)*	1.23 (1.16–1.44)*	1.2 (0.64–1.3)*	1.39 (1.3–1.52)* ‡	0.61 (0.54–1.4)*	1.5 (1.5–1.6)* ‡
CBT_{max}, mm	1.18 (0.92–1.26)	1.58 (0.75–1.63)*	1.63 (1.57–1.68)*‡	1.58 (0.88–1.65)*	1.68 (1.58–1.74)*‡	1.0 (0.84–1.68)*	1.82 (1.74; 1.82)*‡
SII (ratio)	228 (217–250)	388 (370–428)*	428 (399–464)*‡	434 (424–672)*	448 (397–526)* ‡	513 (472–552)*	538 (508–599)*‡
SIRI (ratio)	0.435 (0.410–0.526)	0.53 (0.48–0.64)*	0.55 (0.5–0.81)* ‡	0.56 (0.53–0.62)*	0.64 (0.54–0.98)*‡	0.62 (0.62–0.82)*	1.1 (0.98–1.14)*‡
AISI (ratio)	75 (68–91)	102 (93–117)*	107 (101 –189)*‡	112 (105 –309)*	127 (103 –239)*‡	212 (194 –261)*	249 (222 –267)*‡
IOP, mm Hg	15 (14–17)	33 (32–38)*	33 (32–38)*	33 (29–40)*	33 (33–40)*	40 (37–42)*	40 (36–42)*

Note: IQR, interquartile range; max, maximum value; Me, median; *, difference between controls and PDR/RVO group, $p < 0.05$; ‡, difference between DRP and RVO for the particular Weiss grade, $p < 0.05$;
Abbreviations: AISI, Aggregate Index of Systemic Inflammation; CBT_1, ciliary body thickness at a point 1-mm posterior to the sclera spur; CBT_{max}, maximum ciliary body thickness; IOP, intraocular pressure; NVG, neovascular glaucoma; PDR, proliferative diabetic retinopathy; RVO, retinal vein occlusion; SII, Systemic Immune Inflammation Index; SIRI, Systemic Inflammation Response Index

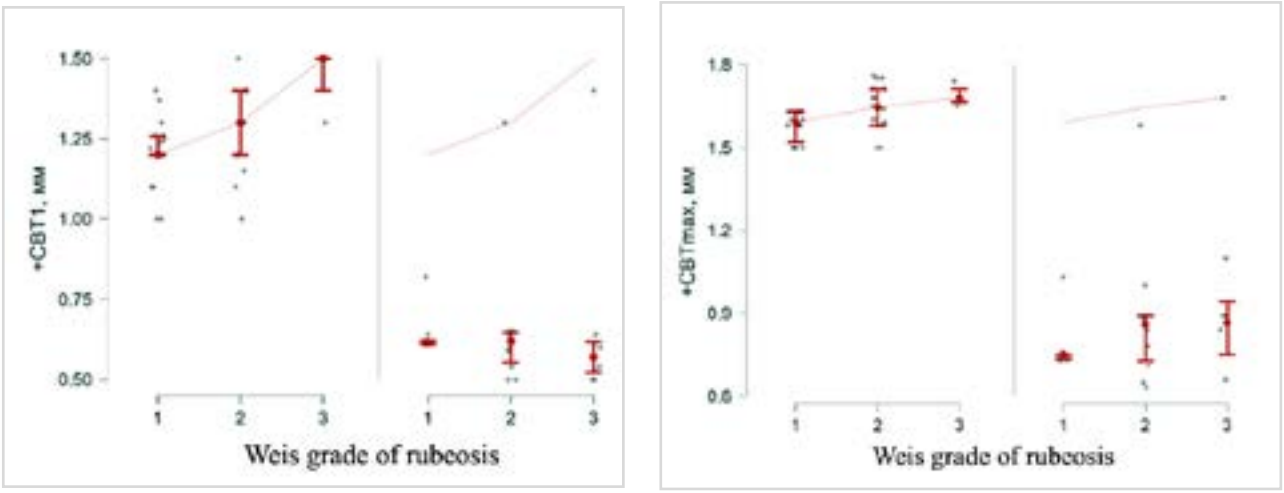

Fig. 2. Relationship between ciliary body thickness (CBT1 and CBTmax), rubeosis grade and PDR duration (A, PDR duration ≤ 5 years; B, PDR duration > 5 years).

phenotype prevails in early disease, but exhibits a transition into an atrophic phenotype with disease progression and increase in disease duration. Additionally, the results obtained suppose that, in eyes with NVG due to RVO, CB thickening is more marked and is maintained under conditions of acute or subacute process after RVO (median duration, 15 (13–21) months).

Systemic immune inflammation indices (SII, SIRI, AISI)

In patients with NVG, all integral indices of systemic inflammation were significantly increased compared to controls, and showed a steady increase with an increase in the Weiss grade of rubeosis (Table 1). The levels of SII and AISI were about 40-90% higher in early NVG compared to controls, indicating early activation of a cascade of systemic immune inflammation.

The severity of the inflammatory component increased with an increase in the Weiss grade of rubeosis, and in rubeosis grades 2-3, SII was twice higher, AISI was 2.5–3.0-fold higher, and SIRI was 1.3–2.0-fold higher compared to controls, and all these differences were significant. Integral indices of systemic immune inflammation were at average 10-25% higher in NVG due to RVO than in the same stage of NVG due to PDR, which reflects a more intensive systemic inflammation component in the former form of NVG.

Therefore, in the current study, indices of systemic immune inflammation demonstrated a relationship with the grade of neovascular process, and allow quantitatively characterizing the etiological differences of the course of NVG in addition to morphometric characteristics of the CB (Table 1).

The level of IOP statistically significantly increased with an increase in the Weiss grade of rubeosis, and was highest in late NVG irrespective of etiology. Spearman rank correlation analysis was conducted to assess correlations between IOP, morphometric characteristics of the CB and indices of systemic immune inflammation.

After stratification for etiology, correlations between morphometric characteristics of the CB and clinical and biological characteristics were stronger in patients with NVG due to RVO than in patients with NVG due to PDR ($p < 0.05$).

In NVG due to RVO, CBT1 showed a positive moderate correlation with SIRI (rs = 0.48), AISI (rs = 0.43) and SII (rs = 0.40). A weaker correlation between CB thickness and these indices was observed in NVG due to PDR (SIRI (rs = 0.46), SII (rs = 0.37) and AISI (rs = 0.36).

Additionally, in a total sample of patients with NVG, the Weiss grade of rubeosis was statistically significantly correlated with the IOP (rs = 0.53), but was stronger correlated with CBTmax (rs = 0.64) and CBT1 (rs = 0.71). IOP showed a positive moderate correlation with CBTmax (rs = 0.49). We found a close correlation between CBT1 and CBTmax (rs = 0.70), which (1) confirms that they are consistent with each other and (2) reflects a uniform process of structural and functional remodeling of the CB in NVG (Fig. 3).

In patients with NVG due to PDR, CBT1 and CBTmax were apparently negatively correlated with the duration of PDR (rs = –0.65 and rs = –0.69, respectively), and these morphometric characteristics decreased with an increase in disease duration ($p < 0.05$). These findings suppose the presence of a time-dependent transition from a swelling-hypervoluminous phenotype to an atrophic phenotype with disease progression.

A multifactorial linear regression analysis was performed to identify independent predictors of CB thickening and to assess quantitatively the contribution of systemic inflammation into the morphometric changes in the anterior segment in NVG. CBTmax was used as a dependent variable. The model also included the clinical parameter (IOP), the local morphometric characteristic (CBT1), systemic immune inflammation indices (SII, SIRI, AISI), and nosological affiliation with the NVG group (Table 2).

Our multivariate regression analysis found the strongest of the maximum cliary body thickness CBTmax to be the systemic immune inflammation indices. In the basic model, ($R2 = 0.23$; $R2adj = 0.20$; $p < 0.001$), SIRI ($\beta = 0.52$; $p < 0.001$), AISI ($\beta = –0.72$; $p < 0.001$) and CBT1 ($\beta = 0.32$; $p = 0.004$) were independent predictors of, whereas IOP and SII had no statistically significant effect on, the dependent variable CBTmax. With the inclusion of the "nosological affiliation with the NVG group" variable into the model, the explaining capacity of the model increased R2 = 0.38; R2adj = 0.34; $p < 0.001$), and the variable became the strongest independent predictor ($\beta = 0.43$; $p < 0.00001$).

This indicated that morphometric changes in the CB in NVG are caused mostly by the systemic inflammatory and

Table 2. Results of multivariate linear regression analysis of predictors of maximum ciliary body thickness (CBT_{max})

Variable	Model 1 β (p)	Model 2 β (p)
IOP	–0.05 (0.64)	–0.04 (0.65)
SIRI	0.52 (0.0001)	0.34 (0.007)
SII	–0.01 (0.93)	–0.04 (0.80)
AISI	–0.72 (0.0002)	–0.49 (0.006)
CBT_1, mm	0.32 (0.004)	0.15 (0.15)
Affiliation with NVG group	–	0.43 (<0.00001)
R^2	0.23	0.38
Adjusted R^2	0.20	0.34
F, p	7.26; <0.001	11.95; <0.001

Notes: Model 1, multivariate linear regression model not taking into account the affiliation with the NVG group; Model 2, multivariate linear regression model taking into account the affiliation with the NVG group; β, standardized regression coefficient; R^2, determination coefficient; adjusted R^2, adjusted determination coefficient; F, Fisher test value; p, P-value. Abbreviations: AISI, Aggregate Index of Systemic Inflammation; CBT_1, ciliary body thickness at a point 1-mm posterior to the sclera spur; CBT_{max}, maximum ciliary body thickness; IOP, intraocular pressure; NVG, neovascular glaucoma; SII, Systemic Immune Inflammation Index; SIRI, Systemic Inflammation Response Index

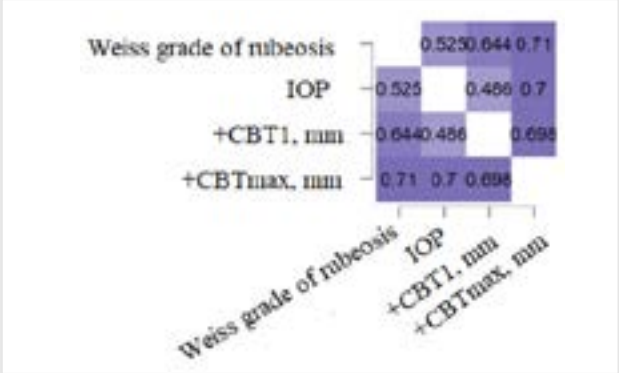

Fig. 3. Heat map of Spearman's correlations between the Weiss grade of rubeosis, intraocular pressure (IOP) and morphometric parameters of the ciliary body (CBT1 and CBTmax) for controls vs the group of ciliary body morphometry. The heat map translates the Spearman's correlation into an easily visualized data set depicting the magnitude and direction of correlations. All the correlations presented are significant ($p < 0.001$).

neovascular components, whereas the IOP is not an independent determinant of CB thickening.

Spearman's rank correlation, but not the multivariate regression model demonstrated a significant correlation of the IOP with the dependent variable CBTmax. This discrepancy indicates that the association of the IOP with the CBTmax is indirect, and likely is mediated by the effect of systemic inflammation and nosological affiliation with the NVG group.

No major violations of linear regression assumptions were observed, there were no signs of significant multicollinearity (Variance Inflation Factors < 3), the standardized residuals were normally distributed (Shapiro–Wilk $p > 0.05$), and the Durbin–Watson factor was 1.47, indicating no clinically significant autocorrelation.

The correlations obtained confirmed our hypothesis on the existence of a uniform structure-and- inflammation axis in NVG, with systemic inflammation, rubeosis grade and morphological changes in the anterior segment being in close interaction with each other.

Discussion

In diabetes, CB edema develops due to combined effect of diabetic microangiopathy, anterior segment ischemia, endothelial dysfunction and activation of systemic immune inflammation, which is accompanied by increased vascular permeability and interstitial transudation in the presence of endothelial dysfunction and increased pro-inflammatory mediators with the involvement of VEGF and adhesion molecules [25]. Under these conditions, CB thickness and volume increase, which reflects the development of swelling-hypervoluminous morphological changes [26], and UBM demonstrates high sensitivity of the ciliary body to ischemia, inflammation and vascular abnormalities [7]. This process has a complex structural and functional nature; this is clearly visualized by UBM that directly assesses the morphology of the CB [23] even in the presence of cloudy or opaque optical media [27].

In NVG, UBM has major advantages over other anterior segment imaging modalities, enabling enables high-resolution imaging of the ciliary region, reliable quantitative evaluation of CB parameters, and the possibility of assessing structural changes under conditions of marked ischemia or neovascularization [7]. The technique enables visualizing the structures of the iridocorneal angle and CB even in difficult clinical conditions, when optic imaging techniques are of limited use [28]. The UBM measurements of the CB may have a prognostic value, e.g., for assessing the efficacy of trans-scleral diode cyclo-photocoagulation [29].

Chronic hyperglycemia results in reduced capillary perfusion and reduced intraocular blood flow [30]. Local anterior segment ischemia results in increased vascular permeability and the development of interstitial stromal edema of the CB [7]. The ischemic lesion is accompanied by activation of VEGF- signaling pathways and pro-inflammatory cascade with increased expressions of IL-6, TNF-α [30] and the molecular marker of intracellular adhesion (ICAM-1), resulting in endothelial barrier breakdown and increased plasmatic transudation [30, 32]. As a result, these processes are associated with increases in CB thickness and volume [26].

Inflammation is a key pathogenetic mechanism in RVO and diabetic lesions, which is implemented through the activation of pro-inflammatory and pro-angiogenic cytokines (IL-6, TNF-α, IL-1β, and VEGF), microvascular dysfunction, vasogenic edema and progression of neovascularization [33, 34]. Studies demonstrated a direct relationship between the levels of pro-inflammatory factors and severity of macular edema in RVO [35] and the role of systemic inflammation in clinical outcomes of secondary macular edema [36].

These mechanisms are especially important in NVG, because RVO is a major cause of ischemic NVG. In the current study, in NVG secondary to RVO, CB morphometry was most strongly associated with systemic immume inflammation indices (the coefficient of rank correlation was $rs = 0.65$ for the correlation of CBT1 with SIRI, and $rs = 0.63$ for the correlation with the Weiss grade of rubeosis). This indicates close association between systemic inflammation, activity of neovascularization and morphological changes in the anterior segment.

In PACG, CB thickness is low, with a CBT1 of 0.56–0.57 mm and CBTmax of 0.87 mm, which corresponds to a more compact morphological phenotype of the CT [27]. These characteristics are higher in healthy individuals (CBT1= 0.81 mm; CBTmax= 1.25 mm), which reflects the physiological status of the CB [9].

The morphometric profile of the CB in eyes with NVG is principally different from those in normal eyes or eyes with PACG. In the current study, CB thickness in eyes with NVG secondary to RVO and eyes with NVG secondary to PDR with duration of diabetes ≤ 5 years exceeded those in normal eyes or eyes with PACG: the CBT1 ranged within 1.17–1.50 mm, and the CBTmax was as much as 1.64 mm. These values are actually twice as high as normal values, supposing the formation of a hypervoluminous phenotype of the CB. Reactive morphometric changes in the CB after vitrectomy with gas or silicone tamponade have been described, confirming a high sensitivity of the CB to impaired microcirculation and effects of inflammation [36].

The results of our multivariate regression analysis confirmed independent contributions of systemic inflammation in the formation of morphological changes in the CB. The adjusted determination coefficient (R^2adj) was 0.20 in the basic model, increasing to 0.34 with the inclusion of the "nosological affiliation with the NVG group" variable into the model; this accounted for a 20–34% in the variability of CBTmax. SIRI ($\beta = 0.34$; $p < 0.01$) and AISI ($\beta = –0.49$; $p < 0.01$) remained independent predictors of CB thickening, whereas the IOP had no statistically significant effect.

Similar values of the coefficient of determination have been reported by other studies on the morphometry of the anterior segment in eyes with PACG or retinal vascular lesions, with an explaining capacity of multifactorial models

usually not exceeding 0.30–0.35 [9, 21, 38]. This confirms that, under conditions of the multicomponent pathogenesis of NVG, this level of explaining capacity is methodologically grounded and clinically interpretable.

Thinning of the CB to the values close to the lower normal range or even the values typical for PACG (CBT1 = 0.57–0.64 mm; CBTmax = 0.74–1.00 mm) was observed in NVG secondary to PDR with a duration > 5 years. This supposes that a swelling-hypervoluminous phenotype exhibits a transition into an atrophic phenotype of the CB due to chronic ischemia, progressive miscrovascular obliteration and durable systemic low-grade inflammation.

Therefore, thinning or thickening of the CB in secondary NVG may be considered an integral marker of the ischemic-and-inflammatory processes implemented through local microcirculatory abnormalities and neovascularization and may play a role in the formation of a clinical course of the disease.

Conclusion

First, in eyes with NVG, the UBM thickness of the CB varies widely, depending on the etiology and disease duration, with the greatest median values observed in NVG secondary to RVO and NVG secondary to DR with a duration ≤ 5 years (CBT1, 1.25–1.39 mm; CBTmax, 1.63–1.66 mm). These values are actually twice as high as normal values, supposing the formation of a hypervoluminous inflammatory-swelling phenotype of the CB. An abrupt thinning of the CB (CBT1 = 0.57–0.64 mm; CBTmax = 0.74–1.00 mm), indicating a likely atrophic transformation, was observed in NVG secondary to PDR with a duration > 5 years.

Second, in NVG, systemic immune-inflammation indices (SII, SIRI, and AISI) showed a significant steady increase with an increase in the Weiss grade of rubeosis and demonstrated a close association with the morphometry of the CB. In rubeosis grades 2-3, SII was twice higher, AISI was 2.5–3.0-fold higher, and SIRI was 1.3–2.0-fold higher compared to controls, reflecting grade-to-grade changes in the systemic inflammation component of NVG.

Finally, the results of our multivariate regression analysis confirmed independent contributions of systemic inflammation in the formation of morphological changes in the CB: SIRI and AISI were still statistically significant after adjustment for clinical and morphometric factors. This indicates that, in NVG, structural changes in the CB are associated with the ischemic-and-inflammatory pathogenetic cascade and play a role in the formation of a clinical course of the disease.

Author contributions

OG, OZ, VS, NK and OK contributed to Conceptualization, Study Design, Data Collection, Analysis and Interpretation of Results and Manuscript Preparation.

Funding

This paper is a part of the 2019-2021 research program "To examine the features of changes in anterior segment structures, blood flow and heat exchange in neovascular glaucoma and trauma (registration number № 0119U101215)".

Conflict of interest

The authors state that they have no conflict of interest that could influence their view on the subject matter or materials described and discussed in this manuscript.

Acknowledgement

The authors are grateful to Professor Andrii Korol, Deputy Director for International Work, for his support in performing this study and writing this article.

Data Availability Statement

All the data obtained or examined during this study has been incorporated into this published article. The datasets generated and/or analyzed during the current study are available from the corresponding author on reasonable request.

Abbreviations

AISI, Aggregate Index of Systemic Inflammation; CB, ciliary body; CBT1, ciliary body thickness at a point 1-mm posterior to the sclera spur; CBTmax, maximum ciliary body thickness; DR, diabetic retinopathy; ICAM-1, intercellular adhesion molecule 1; IOP, intraocular pressure; LYM, lymphocytes (×109 /l); MON, monocytes (×10^9 /l); NEU, neutrophils (×10^9 /l); NVG, neovascular glaucoma; PDR, proliferative diabetic retinopathy; PLT, platelets (×10^9 /); RVO, retinal vein occlusion; SII, Systemic Immune-Inflammation Index; SIRI, Systemic Inflammation Response Index; UBM, ultrasound biomiscroscopy; VEGF, vascular endothelial growth factor

References

1. Hayreh SS. Neovascular glaucoma. Prog Retin Eye Res. 2007 Sep;26(5):470-85. doi: 10.1016/j.preteyeres.2007.06.001.
2. Dumbrăveanu L, Cușnir V, Bobescu D. A review of neovascular glaucoma. Etiopathogenesis and treatment. Rom J Ophthalmol. 2021 Oct-Dec;65(4):315-329. doi: 10.22336/rjo.2021.66.
3. Guzun O, Zadorozhnyy O, Chargui W. Modern strategy for the treatment of neovascular glaucoma secondary to ischemic retinal lesions [in Ukrainian]. Journal of Ophthalmology (Ukraine). 2024;2(517):32–39.
4. Zett C, Stina DMR, Kato RT, Novais EA, Allemann N. Comparison of anterior segment optical coherence tomography angiography and fluorescein angiography for iris vasculature analysis. Graefes Arch Clin Exp Ophthalmol. 2018 Apr;256(4):683-691. doi: 10.1007/s00417-018-3935-7.
5. Zadorozhnyy O, Alibet Y, Kryvoruchko A, Levytska G, Pasyechnikova N. Dimensions of ciliary body structures in various axial lengths in patients with rhegmatogenous retinal detachment. J Ophthalmol (Ukraine). 2017;6:32-35. doi.org/10.31288/oftalmolzh201763236
6. Kovalchouk AG. Substantiating the potential for a new technique (impedance oculopneumoplethysmography) to assist in diagnosing microvascular ciliary body ischemia. Oftalmol Zhurn. 2018;38(3):85-97. doi.org/10.31288/oftalmolzh201838597
7. Warjri GB, Senthil S. Imaging of the Ciliary Body: A Major Review. Semin Ophthalmol. 2022 Aug;37(6):711-723. doi: 10.1080/08820538.2022.2085515.
8. Yousef YA, AlNawaiseh I, AlShawaqfeh MS, Alomari A, Al-Dolat W, AlBdour M. Ultrasound biomicroscopy measurements of the normal thickness of the ciliary body and iris. J Clin Med. 2022;11(9):2483. doi:10.3390/jcm11092483.
9. Ren J, Wu H, Zhang H, Li M, Wang N, Chen X. Characteristics of the ciliary body in healthy subjects quantified by

ultrasound biomicroscopy. J Clin Med. 2022;11(13):3696. doi:10.3390/jcm11133696.
10. Guo L, Liu Y, Huang X, Liu Q, Shen Z, Wu Y, Yang L. Anterior segment features in neovascular glaucoma: An ultrasound biomicroscopy study. Eur J Ophthalmol. 2025 Jan;35(1):214-220. doi: 10.1177/11206721241252476.
11. Nongpiur ME, He M, Amerasinghe N, Friedman DS, Tay WT, Baskaran M, Smith SD, Wong TY, Aung T. Lens vault, thickness, and position in Chinese subjects with angle closure. Ophthalmology. 2011 Mar;118(3):474-9. doi: 10.1016/j.ophtha.2010.07.025.
12. Sun X, Dai Y, Chen Y, Yu DY, Cringle SJ, Chen J, et al. Primary angle closure glaucoma: What we know and what we don't know. Prog Retin Eye Res. 2017 Mar;57:26-45. doi: 10.1016/j.preteyeres.2016.12.003.
13. Bulu A, Keser S. The relationship between pan-immune inflammation value and different stages of diabetic retinopathy in patients with type 2 diabetes mellitus: a prospective cross-sectional study. BMC Endocr Disord. 2025 Jul 23;25(1):184. doi: 10.1186/s12902-025-02007-x.
14. Deng R, Zhu S, Fan B, Chen X, Lv H, Dai Y. Exploring the correlations between six serological inflammatory markers and different stages of type 2 diabetic retinopathy. Sci Rep. 2025 Jan 10;15(1):1567. doi: 10.1038/s41598-025-85164-2.
15. Gong Y, Wang L, Li Q, et al. Evaluating neutrophil-lymphocyte ratio, systemic immune-inflammation index, and systemic inflammation response index for diagnosing and predicting progression in diabetic retinopathy: a cross-sectional and longitudinal study. BMC Ophthalmol. 2025 Jul 8;25(1):398. doi: 10.1186/s12886-025-04222-5.
16. Jia R, Yin Y, Shan H. Systemic inflammatory response index as a novel biomarker for age-related macular degeneration: a cross-sectional study from NHANES (2005-2008). Front Nutr. 2025 Mar 6;12:1540933. doi: 10.3389/fnut.2025.1540933.
17. Zhang A, Ning L, Han J, et al. Neutrophil-to-lymphocyte ratio as a potential biomarker of neovascular glaucoma. Ocul Immunol Inflammation. 2021;29(2):417].
18. Ogura S, Kurata K, Hattori Y, et al. Sustained inflammation after pericyte depletion induces irreversible blood-retina barrier breakdown. JCI Insight. 2017 Feb 9;2(3):e90905. doi: 10.1172/jci.insight.90905.
19. Bhutia CU, Kaur P, Singh K, Kaur S. Evaluating peripheral blood inflammatory and metabolic biomarkers as predictors in diabetic retinopathy and diabetic macular edema. Indian J Ophthalmol. 2023 Jun;71(6):2521-2525. doi: 10.4103/IJO.IJO_345_23.
20. Harley O, Amelia YS, Gustianty E, Soetedjo NNM, Kartasasmita AS. Exploring leukocyte differential count ratio profiles as inflammatory biomarkers in diabetic retinopathy: a systematic review and meta-analysis. BMC Ophthalmol. 2025 May 1;25(1):265. doi: 10.1186/s12886-025-04075-y.
21. Kazantzis D, Machairoudia G, Kroupis C, Theodossiadis G, Theodossiadis P, Chatziralli I. Complete Blood Count-Derived Inflammation Indices and Retinal Vein Occlusion: A Case-Control Study. Ophthalmol Ther. 2022 Jun;11(3):1241-1249. doi: 10.1007/s40123-022-00511-0.
22. Niu TT, Xiao Y, Lyu WJ, Zhou H. Serologic parameters in young patients with retinal vein occlusion treated with anti-vascular endothelial growth factor. Int J Ophthalmol. 2025 Mar 18;18(3):424-434. doi: 10.18240/ijo.2025.03.09.
23. Li J, Drechsler J, Lin A, Widlus M, Qureshi A, Stoleru G, et al. Repeatability and Reliability of Quantified Ultrasound Biomicroscopy Image Analysis of the Ciliary Body at the Pars Plicata. Ultrasound Med Biol. 2021;47(7):1949–1956. doi:10.1016/j.ultrasmedbio.2021.03.002
24. Weiss D, Gold D. Neofibrovascularization of iris and anterior chamber angle: A clinical classification. Ann Ophthalmol. 1978;10:488–491.
25. Yang DR, Wang MY, Zhang CL, Wang Y. Endothelial dysfunction in vascular complications of diabetes: a comprehensive review of mechanisms and implications. Front. Endocrinol. 2024; 15:1359255. doi: 10.3389/fendo.2024.1359255
26. Kim C Yu HG. Changes in ciliary body thickness in patients with diabetic macular edema after vitrectomy. Retina. 2012 Jul;32(7):1316-23. doi: 10.1097/IAE.0b013e318236e81d.
27. Silverman RH. High-resolution ultrasound imaging of the eye: a review. Clin Exp Ophthalmol. 2009;37(1):54–67. doi:10.1111/j.1442-9071.2008.01892.x.
28. Qin YJ, Luo FL, Zeng J, Zhang YL, Xie WJ, Chen YL, et al. Thinning of maximum ciliary body thickness: a potential early indicator for pseudophakic malignant glaucoma in primary angle closure glaucoma. BMC Ophthalmol. 2025;25(1):250. doi:10.1186/s12886-025-04100-0.
29. Safwat AMM, Hammouda LM, El-Zembely HI, Omar IAN. Evaluation of ciliary body by ultrasound bio-microscopy after trans-scleral diode cyclo-photocoagulation in refractory glaucoma. Eur J Ophthalmol. 2020 Nov;30(6):1335-1341. doi: 10.1177/1120672119899904.
30. Guzun OV, Zadorozhnyy OS, Velychko LM, Bogdanova OV, Dumbrăveanu LG, Cuşnir VV, et al. The effect of intercellular adhesion molecule-1 and glycated haemoglobin on the management of diabetic neovascular glaucoma. Rom J Ophthalmol. 2024;68(2):135–142. doi:10.22336/rjo.2024.25.
31. Campochiaro PA. Ocular neovascularization and excessive vascular permeability. Prog Retin Eye Res. 2020;78:100847. doi:10.1016/j.preteyeres.2020.100847
32. Noma H, Yasuda K, Shimura M. Cytokines and inflammatory factors in retinal vascular diseases. Prog Retin Eye Res. 2019;70:1–27. doi:10.1016/j.preteyeres.2018.11.001
33. Noma H, Yasuda K, Shimura M. Cytokines and Pathogenesis of Central Retinal Vein Occlusion. J Clin Med. 2020 Oct 27;9(11):3457. doi: 10.3390/jcm9113457.
34. Siqueira RC, Brandão CC. The Role of Cytokines in Degenerative Retinal Diseases: A Comprehensive Review. Biomedicines. 2025;13(7):1724. doi:10.3390/biomedicines13071724.
35. Noma H, Mimura T, Eguchi S. Association of Inflammatory Factors With Macular Edema in Branch Retinal Vein Occlusion. JAMA Ophthalmol. 2013;131(2):160–165. doi:10.1001/2013.jamaophthalmol.228
36. Böhm EW, Wolfrum P, Welzel AM, Schuster AK, Wagner FM, Gericke A, et al. Systemic inflammation in retinal vein occlusion and its role in clinical outcomes of secondary macular edema. J Clin Med. 2026;15(2):407. doi:10.3390/jcm15020407.
37. Ünsal E, Eltutar K, Karini B, Kızılay O. Assessment of Anterior Segment Changes in Pseudophakic Eyes, Using Ultrasonic Biomicroscopic Imaging, after Pars Plana Vitrectomy with Silicone Oil or Gas Tamponade. J Ophthalmol. 2016;2016:8303792. doi: 10.1155/2016/8303792.
38. Chen SY, He N, Yan YJ, Fan X, Wu LL. Ultrasound biomicroscopic imaging demonstrate thinner ciliary body thickness in eyes with angle closure. Int J Ophthalmol. 2022 Sep 18;15(9):1476-1482. doi: 10.18240/ijo.2022.09.10.